

SYNTHESIS OF DIHYDROTETRAZOLOPYRIMIDINE DERIVATIVES AS ANTICANCER AGENTS AND INHIBITOR OF α -GLUCOSIDASE

H. Suwito^{1,✉}, N. Kurnyawaty³, K.U. Haq^{1,2}, R. Ramadhan^{1,2}, A. Abdulloh¹, H.D. Hardiyanti¹ and P. Phuwapraisirisan⁴

¹Department of Chemistry, Faculty of Science and Technology, Universitas Airlangga, Surabaya-60115, Indonesia

²University of CoE-Research Center for Bio-Molecule Engineering (BIOME), Universitas Airlangga, Surabaya-60115, Indonesia.

³Department of Chemical Engineering, State Polytechnic of Samarinda, Samarinda-75131, Indonesia

⁴Department of Chemistry, Faculty of Science, Chulalongkorn University, Bangkok-10330, Thailand

✉Corresponding Author: hery-s@fst.unair.ac.id

ABSTRACT

A series of dihydrotetrazolopyrimidine derivatives were prepared to utilize a three-component Biginelli reaction from ethyl 3-oxo butanoate, 5-amino tetrazole, and various aromatic aldehydes as reactants, pTSA as a Brønsted acid catalyst, and ethanol as the solvent. The structure of the prepared compounds was established by spectroscopic evidence, FTIR, HRMS, and NMR (¹H- and ¹³C-) spectra. The electronic properties of the aromatic aldehyde's substituents affected the reaction's time and yield. Substituents possessing electron-donating character accelerated the reaction time but decreased the reaction yield, whereas substituents with electron-withdrawing properties slowed the reaction but increased the yield. The prepared compounds exhibited moderate to strong anti-proliferative activities against 4T1 and HeLa cancer cell lines. Compound Ethyl (*E*)-5-methyl-7-(1-phenylprop-1-en-2-yl)-4,7-dihydrotetrazolo[1,5-a]pyrimidine-6-carboxylate and compound Ethyl 7-(1H-indol-3-yl)-5-methyl-4,7-dihydrotetrazolo[1,5-a]pyrimidine-6-carboxylate showed strong anti-proliferative activities in vitro through induction apoptotic cells death mechanism. In addition, five of the synthesized compounds exhibited better inhibitory activity of α -glucosidase than quercetin, the positive control.

Keywords: Dihydrotetrazolopyrimidine, Biginelli Reaction, Anticancer, Apoptosis, Anti-Diabetes.

RASAYAN J. Chem., Vol. 16, No.1, 2023

INTRODUCTION

Cancer remains a high-risk global health problem, the second-highest cause of death, and the predicted primary cause of death in the future.¹ According to American Cancer Society², over 1,9 million new cancer cases are expected to be diagnosed in the US in 2022, while 609,360 deaths from cancer are expected. A significant enhancement of economic impact follows this. The annual economic cost of cancer in 2010 was estimated at US\$ 1.16 trillion, nearly 19 percent higher than heart disease.² Although the development of various treatment strategies is continuously ongoing, relapses and treatment-related complications remain a hindrance. In cancer chemotherapy, the applied anticancer drugs generally act as cytotoxic agents, associated with various side effects, working on an unspecified target, and marred by drug resistance.^{3,4} Related to the management of cancer therapy, utilization of anticancer drugs working through apoptotic cell death mechanism is preferred due to the ease of follow-up care.⁵ Therefore, discovering small molecules that exhibit potent and selective anticancer activities is still a goal and challenge in medicinal chemistry research. Diabetes mellitus is considered a serious health problem worldwide due to enhancing occurrence rate indicated by the increasing obesity and aging of the population. The global diabetes prevalence in 2021 was estimated to be 536.6 million people, rising to 783.2 million in 2045.⁶ Two types of diabetes mellitus are known, type-1 is insulin-dependent diabetes mellitus, while type-2 is non-insulin-

dependent diabetes mellitus. Generally, diabetes mellitus is characterized by a disorder of carbohydrate, protein, and fat metabolism due to complete or partial inadequacy of insulin action and/or insulin secretion⁷ and by high blood glucose levels.⁸ The central pathophysiology of diabetes is pancreatic β -cells and insulin as its secretory product. However, various pathogenic mechanisms for developing hyperglycemia are determined.⁷ Chronic hyperglycemia due to partial or complete deficiencies in insulin secretion is a characteristic symptom of type-2 diabetes. Prolonged postprandial hyperglycemia leads to uncontrolled high blood glucose levels and the formation of cytotoxic non-enzymatic glycation products in various tissues as a cause of complications of diabetes.⁹ In addition, prolonged postprandial hyperglycemia also leads to glucose autooxidation, and overproduction of free radicals is also observed.^{10,11} The α -glucosidase (α -Gls) is an essential enzyme in polysaccharides, and disaccharides break down into glucose.¹² Therefore, one therapeutic strategy to control postprandial hyperglycemia is retarding glucose absorption through inhibition of α -glucosidase (α -Gls) as shown by various antidiabetic drugs, such as voglibose and acarbose.^{12,13} Furthermore, the α -Gls is a notable target for inhibition by antiviral agents¹⁴ and anticancer.¹⁵ However, molecular structures of most of the known constructed glucosidase inhibitors are usually carbohydrate mimics, which need long multi-step reaction pathways, both from sugar and non-sugar sources. These commonly applied α -Gls inhibitors show several disadvantages, such as low efficacy with high IC_{50} value¹⁶, and sometimes are associated with the appearance of rare adverse hepatic events.¹⁷ In addition, none of these antidiabetic drugs can treat the cause of diabetes. The Biginelli reaction is a one-pot multi-component reaction of a 1,3-dicarbonyl compound, urea, and benzaldehyde to furnish 3,4-dihydropyrimidine derivatives.^{18,19} In addition to the versatility of the reaction components, the Biginelli reaction is also of interest as molecular structures of its various reaction products can be predicted. The use of 5-amino tetrazole replacing urea as a building block to form dihydro-tetrazolopyrimidine possessing a purine ring is one example of the versatility of this reaction.²⁰ Derivatives of dihydrotetrazolopyrimidine have also shown various biological activities, particularly antimicrobial²¹, hypoglycemic and antibacterial²², antioxidant²³, anticancer²⁴, hyperuricemic²⁵, an inhibitor of HIV gp-120-CD4²⁶ activities. Moreover, it has been demonstrated that various purine derivatives possess potent antituberculosis activity.²⁷ In the present study, we aimed to design and synthesize small molecules derivatives of dihydrotetrazolo pyrimidine both as anticancer small molecules and as anti-diabetic agents via a convenient Biginelli reaction. Based on the literature study, the prepared compounds' anticancer and α -Gls inhibitory activities were not reported yet. Furthermore, we studied the apoptosis-inducing mechanism and cell cycle of the two most anticancer-potent compounds. The anti-diabetic activity was assessed by inhibition of α -Glucosidase assay. The mechanism of inhibition activity was then studied through molecular interaction of the most active compound by docking experiment toward α -glucosidase of *Mus musculus* accessed from Protein Data Bank.

EXPERIMENTAL

Materials

All reagents used were of synthesis grade and provided by Sigma-Aldrich (St. Louis, MO, USA). All solvents used were of pro-analysis grade provided by E. Merck (Darmstadt, Germany) and used without prior purification. Reaction progress and product purity were measured by chromatography (TLC) on silica aluminum plates (0.25 mm) with a fluorescent coating (E. Merck, Darmstadt, Germany) using various solvents as a mobile phase.

Instrumentation

TLC spots were visualized using a UV lamp (Sankyo Denki O8T5, Japan; $\lambda = 254$ nm). An infrared spectrophotometer (Shimadzu, Kyoto, Japan; IRTracer-100) was used to record the FTIR spectra in KBr powder by the diffuse reflectance method, and bands were expressed in wave number (cm^{-1}). Mass spectra were obtained using an HRMS (Water LCT Premier XE; Santa Clara, California, USA). NMR spectra were obtained on a 400 MHz JEOL JNM-ECS400 spectrometer (Tokyo, Japan) using $CDCl_3$ or $DMSO-d_6$ as solvents and an internal standard. A microplate reader Tecan (Infinite F50, Tecan Trading AG, Switzerland), was employed to perform the α -glucosidase inhibition assays. A flow cytometer BD FACS Calibur (San Jose, CA, USA) was used for cell cycle and apoptosis evaluation.

Synthesis of Target Molecules

5-amino tetrazole (6 mmol), aromatic aldehydes (5 mmol), ethyl acetoacetate (5 mmol), *para*-toluene sulfonic acid (1 mmol), and ethanol (3 ml) were poured consecutively into a reaction flask, then refluxed to the completion of the reaction (monitored chromatographically). The mixture was then subsequently cooled and separated by filtration. The product was cleaned using cold ethanol and recrystallized. The structures of the reaction products were determined based on spectroscopic evidence by FTIR, HRMS, ¹H- and ¹³C-NMR. Briefly, spectroscopic data of the prepared compounds are displayed below.

Ethyl 7-(2,4-dimethoxyphenyl)-5-methyl-4,7-dihydrotetrazolo[1,5-a]pyrimidine-6-carboxylate (1): yellow solid (0.79 g; 45.91%), $R_f=0.51$ (2:1 dichloromethane / ethyl acetate); HR-MS $[M-H]^+$ calcd. for $C_{16}H_{18}N_5O_4$ 344.1359, found 344.1360; FTIR (DRS, KBr, $\tilde{\nu}$, cm^{-1}) 3242 (N-H); 3178 (C-H aromatic); 2943 (C-H aliphatic); 1712 (C=O); 1577 (C=C); 1099 & 1276 (C-O ester); ¹H-NMR (400 MHz, $CDCl_3$) δ (ppm) 11.01 (*s*, 1H); 7.24 (*d*, $J=8.3$ Hz, 1H); 6.88 (*s*, 1H); 6.46 (*dd*, $J=8.3$; 2.4 Hz, 1H); 6.43 (*d*, $J=2.4$ Hz, 1H); 4.08 (*q*, $J=7.1$ Hz, 2H); 3.77 (*s*, 1H); 3.73 (*s*, 1H); 2.63 (*s*, 4H), 1.17 (*t*, $J=7.1$ Hz, 3H), ¹³C-NMR (100.1 MHz, $CDCl_3$) δ (ppm) 165.4; 161.5; 158.6; 149.4; 145.9; 130.7; 120.5; 104.4; 99.0; 98.6; 60.4; 56.1; 55.7; 55.5; 19.6; 14.2.

Ethyl 5-methyl-7-(4-morpholinophenyl)-4,7-dihydrotetrazolo[1,5-a]pyrimidine-6-carboxylate (2): Violet needle crystal (1.08 g; 58%), $R_f=0.47$ (2:1 dichloromethane / ethyl acetate); HR-MS: $[M+H]^+$ calcd. for $C_{18}H_{22}N_6O_3$, 371.1832; found 371.1833; FTIR (DRS, KBr, $\tilde{\nu}$, cm^{-1}) 3242 (N-H); 3178 (C-H aromatic); 2943 (C-H aliphatic); 1712 (C=O); 1577 (C=C, aromatic); 1099 & 1276 (C-O ester); ¹H-NMR (400 MHz, $CDCl_3$) δ (ppm) 11.08 (*s*, 1H); 7.25 (*d*, $J=8.8$ Hz, 2H); 6.83 (*d*, $J=8.8$ Hz, 2H); 6.67 (*s*, 1H); 4.05 (*m*, 2H); 3.83 (*t*, $J=4.8$ Hz, 4H); 3.14 (*t*, $J=4.8$ Hz, 4H); 2.67 (*s*, 4H); 1.16 (*t*, $J=7.1$ Hz, 3H), ¹³C-NMR (100.1 MHz, $CDCl_3$) δ (ppm) 165.1; 151.5; 148.8; 145.7; 131.1; 128.3; 115.5; 99.6; 66.9; 60.9; 59.2; 48.9; 19.6; 14.2.²⁸

Ethyl 7-(furan-2-yl)-5-methyl-4,7-dihydrotetrazolo[1,5-a]pyrimidine-6-carboxylate (3): Pale yellow solid (0.66 g; 47.87%), $R_f=0.55$ (2:1 chloroform / ethyl acetate); HR-MS: $[M+H]^+$ calcd. for $C_{12}H_{14}N_4O_3$, 276.1097; found 276.1099; FTIR (DRS, KBr, $\tilde{\nu}$, cm^{-1}) 3394 (N-H); 3161 (C-H aromatic); 2941 (C-H aliphatic); 1712 (C=O); 1570 (C=C); 1099 & 1276 (C-O ester); ¹H-NMR (400 MHz, $DMSO-d_6$) δ (ppm) 11.34 (*s*, 1H); 7.58 (*d*, $J=1.2$ Hz, 1H); 6.80 (*s*, 1H); 6.45 (*d*, $J=3.1$ Hz, 1H); 6.41 (*dd*, $J=3.2$; 1.4 Hz, 1H); 4.02-4.04 (*m*, 2H); 2.44 (*s*, 3H); 1.10 (*t*, $J=7.1$ Hz, 3H), ¹³C-NMR (100.1 MHz, $DMSO-d_6$) δ (ppm) 164.4; 151.9; 148.6; 147.3; 143.3; 110.8; 108.3; 95.2; 59.7; 52.1; 18.4; 13.9.

Ethyl (E)-5-methyl-7-(1-phenylprop-1-en-2-yl)-4,7-dihydrotetrazolo[1,5-a]pyrimidine-6-carboxylate (4): brown needle crystal (0.19 g; 11.89%), $R_f=0.43$ (2:1 *n*-hexane / ethyl acetate); HR-MS: $[M+H]^+$ calcd. for $C_{17}H_{19}N_5O_2$, 326.1539; found 326.1649; FT-IR (DRS, KBr, $\tilde{\nu}$, cm^{-1}) 3304 (N-H); 3172 (C-H aromatic); 2949 (C-H aliphatic); 1681 (C=O); 1562 (C=C); 1095 & 1290 (C-O ester); ¹H-NMR (400 MHz, $DMSO-d_6$) δ (ppm) 11.18 (*s*, 1H); 7.33 (*m*, 5H); 6.70 (*s*, 1H); 6.23 (*s*, 1H); 3.98-4.04 (*m*, 2H); 2.43 (*s*, 3H); 1.55-1.56 (*m*, 3H); 1.20 (*t*, $J=7.1$ Hz, 3H), ¹³C-NMR (100.1 MHz, $DMSO-d_6$) δ (ppm) 164.7; 149.0; 147.0; 136.1; 134.8; 129.3; 128.8; 128.4; 127.1; 96.1; 62.9; 59.7; 18.4; 14.1; 13.0.

Ethyl 7-(2-methoxyphenyl)-5-methyl-4,7-dihydrotetrazolo[1,5-a]pyrimidine-6-carboxylate (5): White crystal (0.75 g; 47.59%), $R_f=0.57$ (2:1 chloroform / ethyl acetate); HR-MS: $[M+Na]^+$ calcd. for $C_{15}H_{17}N_5O_3Na$, 338.1331; found 338.1221; FTIR (DRS, KBr, $\tilde{\nu}$, cm^{-1}) 3255 (N-H); 3184 (C-H aromatic); 2945 (C-H aliphatic); 1708 (C=O); 1573 (C=C); 1101 & 1278 (C-O ester); ¹H-NMR (400 MHz, $DMSO-d_6$) δ (ppm) 11.17 (*s*, 1H); 7.28 (*t*, $J=7.1$ Hz, 2H); 6.99 (*d*, $J=8.5$ Hz, 1H); 6.92 (*d*, $J=7.5$ Hz, 1H); 6.83 (*s*, 1H); 3.92-3.94 (*m*, 2H); 2.42 (*s*, 3H); 1.03 (*t*, $J=7.1$ Hz, 3H), ¹³C-NMR (100.1 MHz, $DMSO-d_6$) δ (ppm) 164.7; 156.9; 149.0; 146.7; 130.0; 129.5; 128.4; 120.2; 111.8; 96.7; 59.5; 55.6; 55.1; 18.4; 13.7.

Ethyl 7-(4-(dimethylamino)phenyl)-5-methyl-4,7-dihydrotetrazolo[1,5-a]pyrimidine-6-carboxylate (6): Yellow needle crystal (0.69 g; 42.40%), $R_f=0.53$ (2:1 chloroform / ethyl acetate); HR-MS: $[M+Na]^+$ calcd. for $C_{16}H_{20}N_6O_2Na$, 351.1648; found 351.1525; FTIR (DRS, KBr, $\tilde{\nu}$, cm^{-1}) 3232 (N-H); 3169 (C-H aromatic); 2956 (C-H aliphatic); 1697 (C=O); 1575 (C=C); 1099 & 1279 (C-O ester); ¹H-NMR (400 MHz, $CDCl_3$) δ (ppm) 11.12 (*s*, 1H); 7.20 (*d*, $J=8.7$ Hz, 2H); 6.66 (*s*, 1H); 6.66 (*d*, $J=8.7$ Hz, 2H), 4.08-4.09 (*m*,

2H); 2.92 (s, 6H); 2.67 (s, 3H); 1.17 (t, $J=7.2$ Hz, 3H), $^{13}\text{C-NMR}$ (100.1 MHz, CDCl_3) δ (ppm) 165.3; 150.7; 148.9; 145.5; 128.3; 127.7; 112.3; 99.8; 60.5; 59.4; 40.5; 19.6; 14.2.

Ethyl 5-methyl-7-(2,4,6-trimethoxyphenyl)-4,7-dihydrotetrazolo[1,5-a]pyrimidine-6-carboxylate (7): White crystal (0.55 g; 29.45%), $R_f = 0.41$ (2:1 dichloromethane / ethyl acetate); HR-MS: $[\text{M}+\text{Na}]^+$ calcd. for $\text{C}_{17}\text{H}_{21}\text{N}_5\text{O}_5\text{Na}$, 398.1434; found 398.1419; FTIR (DRS, KBr, $\tilde{\nu}$, cm^{-1}) 3248 (N-H); 3180 (C-H aromatic); 2947 (C-H aliphatic); 1705 (C=O); 1577 (C=C); 1128 & 1232 (C-O ester); $^1\text{H-NMR}$ (400 MHz, $\text{DMSO-}d_6$) δ (ppm) 10.97 (s, 1H); 7.06 (s, 1H); 6.18 (s, 2H); 3.92 (q, $J=7.1$ Hz, 2H); 3.74 (s, 6H); 2.54 (s, 3H); 1.04 (t, $J=7.1$ Hz, 3H), $^{13}\text{C-NMR}$ (100.1 MHz, $\text{DMSO-}d_6$) δ (ppm) 165.1; 161.1; 161.1; 149.5; 146.6; 109.3; 96.2; 90.9; 59.2; 55.8; 55.2; 49.2; 18.3; 13.8.

Ethyl 7-(1H-indol-3-yl)-5-methyl-4,7-dihydrotetrazolo[1,5-a]pyrimidine-6-carboxylate (8): White solid (0.04 g; 2.59%), $R_f = 0.36$ (2:1 dichloromethane / ethyl acetate); HR-MS: $[\text{M}+\text{Na}]^+$ calcd. for $\text{C}_{16}\text{H}_{16}\text{N}_6\text{O}_2\text{Na}$, 347.1227; found 347.1220; FTIR (DRS, KBr, $\tilde{\nu}$, cm^{-1}) 3417 (N-H); 3172 (C-H aromatic); 2945 (C-H aliphatic); 1676 (C=O); 1577 (C=C); 1095 & 1315 (C-O ester); $^1\text{H-NMR}$ (400 MHz, $\text{DMSO-}d_6$) δ (ppm) 11.25 (s, 1H); 11.17 (s, 1H); 7.40 (d, $J=2.6$ Hz, 1H); 7.00-7.37 (m, 4H); 6.97 (s, 1H); 3.95-3.97 (m, 2H); 2.46 (s, 3H); 1.13 (t, $J=7.1$ Hz, 3H), $^{13}\text{C-NMR}$ (100.1 MHz, $\text{DMSO-}d_6$) δ (ppm) 164.9; 148.6; 145.4; 136.4; 124.8; 124.7; 121.4; 119.3; 117.9; 114.7; 111.9; 97.8; 59.5; 52.1; 18.2; 13.9.

Ethyl 7-(4-chlorophenyl)-5-methyl-4,7-dihydrotetrazolo[1,5-a]pyrimidine-6-carboxylate (9): White crystal (1.19 g; 74.28%), $R_f = 0.54$ (2:1 chloroform / ethyl acetate); HR-MS: $[\text{M}+\text{Na}]^+$ calcd. for $\text{C}_{14}\text{H}_{14}\text{ClN}_5\text{O}_2\text{Na}$, 342.0836; found 342.0729; FTIR (DRS, KBr, $\tilde{\nu}$, cm^{-1}) 3390 (N-H); 3182 (C-H aromatic); 2912 (C-H aliphatic); 1703 (C=O); 1575 (C=C); 1103 & 1282 (C-O ester); $^1\text{H-NMR}$ (400 MHz, $\text{DMSO-}d_6$) δ (ppm) 11.33 (s, 1H); 7.39-7.42 (m, 2H); 7.37-7.38 (m, 2H); 6.69 (s, 1H); 3.95-3.98 (m, 2H); 2.47 (s, 3H); 1.03 (t, $J=7.1$ Hz, 3H), $^{13}\text{C-NMR}$ (100.1 MHz, $\text{DMSO-}d_6$) δ (ppm) 164.4; 148.3; 146.9; 139.9; 133.1; 129.1; 128.7; 97.2; 59.7; 58.1; 18.5; 13.8.

Ethyl 7-(4-fluorophenyl)-5-methyl-4,7-dihydrotetrazolo[1,5-a]pyrimidine-6-carboxylate (10): White crystal (0.87 g; 58.58%), $R_f=0.53$ (2:1 chloroform / Ethyl acetate); HR-MS: $[\text{M}+\text{Na}]^+$ calcd. for $\text{C}_{14}\text{H}_{14}\text{FN}_5\text{O}_2\text{Na}$, 326.1024; found 326.1027; FTIR (DRS, KBr, $\tilde{\nu}$, cm^{-1}) 3230 (N-H); 3169 (C-H aromatic); 2943 (C-H aliphatic); 1701 (C=O); 1571 (C=C); 1103 & 1228 (C-O ester); $^1\text{H-NMR}$ (400 MHz, CDCl_3) δ (ppm) 11.26 (s, 1H); 7.35-7.37 (m, 2H); 7.02 (t, $J=8.6$ Hz, 2H); 6.72 (s, 1H); 4.09-4.10 (m, 2H); 2.69 (s, 3H); 1.14 (t, $J=7.1$ Hz, 3H), $^{13}\text{C-NMR}$ (100.1 MHz, CDCl_3) δ (ppm) 164.9; 162.9 ($^1J_{\text{CF}}=247.0$ Hz); 148.7; 146.2; 135.8; 129.3 ($^3J_{\text{CF}}=8.4$ Hz); 116.0 ($^2J_{\text{CF}}=21.8$ Hz); 99.2; 60.7; 58.9; 19.7; 14.1.

Anticancer Activity

The prepared compounds' cytotoxicity toward breast cancer cell line 4T1 and cervical cancer cell line HeLa was evaluated via a previously described MTT assay protocol.^{29,30} Doxorubicin was used as a positive control. Cancer cells were collected from the Laboratory of Pathology, Faculty of Medicine, Public Health, and Nursery at Gadjah Mada University, Yogyakarta, Indonesia. Cell lines were cultured in RPMI-1640 containing 10% fetal bovine serum, penicillin, and streptomycin and grown in an incubator (5% CO_2). Cells were seeded in a 96-well plate at a density of 5.0×10^4 cells per well at 37°C , and cells were incubated for 24 h. Then, the tested compounds (7 different concentrations) were added to the cultures and incubated for an additional 24 h. Afterward, 100 μL of MTT solution [50 mg MTT in 10 ml phosphate-buffered saline (PBS)] was added, and cells were further incubated for 4 h at 37°C in 5% CO_2 . To stop the reaction, an equal volume of HCl (0.04 N in isopropanol) was added to each well, followed by the dissolution of the purple formazan by adding 100 μL dimethyl sulfoxide. Formazan was formed proportionately to the total viable cells, of which absorbance was then measured at 570 nm. Experiments were conducted in triplicate. Statistical Probit analysis (SPSS 17) was employed to determine the IC_{50} value. Viability was determined according to the equation:

$$\% \text{ Viable cells} = \frac{\text{Treatment absorbance} - \text{Control medium absorbance}}{\text{Negative Control absorbance} - \text{Control medium absorbance}} \times 100\%$$

Evaluation of Apoptosis and Determination of Cell Cycle using Flow Cytometer

Cancer cells (4T1 and HeLa) were cultured in RPMI medium at a density of 5×10^5 cells/well in 6-well plates and incubated under a 5% CO₂ atmosphere for 24 h. The medium was then washed with PBS. Into each well were added test compounds at IC₅₀ concentrations, then cells were further incubated for 24 h before being suspended in 1 ml cold ethanol and 1 ml PBS. After incubation in a refrigerator for 30 min, the staining reagents (100 µl Annexin V–PI and 350 µl buffer) were added and mixed homogeneously. This mixture was allocated into flow cytometer tubes, and cytograms were evaluated. Cell cycle evaluation was conducted by resuspension of 400 µl homogeneous test solution, followed by incubation for 10 min at 37°C, and reallocation into a flow cytometer tube. The cell cycle profile was then analyzed via flow cytometry. The cell cycle phase was determined using the Cell Quest program.^{31,32}

α -Glucosidase Inhibition Assay

α -glucosidase (maltase and sucrase) from rat intestines was used to evaluate α -glucosidase inhibitory activity following a previously reported protocol.²² Test compounds (10 µl), 20 µl substrate solution (10 mM maltose and 100 mM sucrose in 0.1 M phosphate buffer), crude enzyme (20 µL), and glucose solutions (80 µl) were added consecutively, then incubated for 40 min (for sucrose) or 10 min (for maltose) at 37°C. Glu-kit (Human, Germany) was applied to determine the concentration of glucose released from the reaction mixture based on the glucose-oxidase assay. Quantitative inhibition of enzyme activity was calculated at an absorbance of 503 nm according to the following formula: % Inhibition = $[(A_0 - A_1)/A_0] \times 100$, where A_0 represents the absorbance without a sample, and A_1 represents the absorbance with the sample. The plot of % inhibition of test compounds was used to determine IC₅₀ values.³³

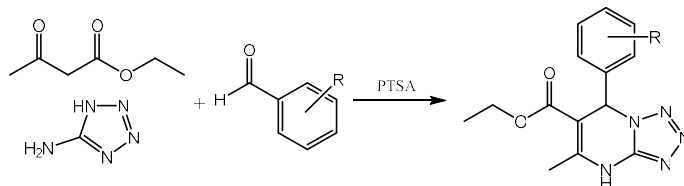
Docking Experiment

Molecular docking was carried out using the Dock 6.8 package. The crystal structure of *Mus musculus* α -glucosidase complexed with Valiolamine was obtained from Protein Data Bank (PDB: 7K9Q).³⁴ Structure preparation and molecular surface generation were conducted by Dock Prep and Write DMS features on Chimera 1.16 package.³⁵ Spheres of the molecular surface were generated using the SPHGEN program, and spheres were selected 8.0 around ligand position using the SPHERE_SELECTOR program. The SHOWBOX program generated a box around the selected sphere with an 8.0 Å extra margin in all directions. Grid was generated in 0.25 Å resolution with the GRID program. In this experiment, Van der Waals interactions were modeled with Lennard-Jone's potential with 6-12 attractive and repulsive exponents. Coulomb potential was used to model the electrostatic interaction with a distance-dependent dielectric coefficient of $\epsilon=4r$.³⁶ The assessment of the docking parameter was validated by the pose reproduction experiment, where the value of the corrected symmetry root means square deviation of the heavy atom (HA_RMSDh) should be less than 2.0 Å. All ligand structures were optimized with MMFF using the Avogadro program³⁷, and the electrostatic charge was computed with the AM1-BCC method using the ANTECHAMBER program.³⁸ The pose of docked ligands was visualized in Maestro 2020 (Schrodinger, Inc.)

RESULTS AND DISCUSSION

Chemistry

A series of dihydrotetrazolopyrimidine compounds 1–10 was synthesized as outlined in Scheme 1. The preparation of target molecules employed the Biginelli reaction, a three-component reaction between ethyl acetoacetate, 5-amino tetrazole, and various aromatic aldehydes using *p*TSA as a Brønsted acid catalyst and ethanol as solvent, conducted under reflux. The reaction progress was measured by TLC and stopped when all reagents had reacted completely. The molecular structures of prepared compounds are presented in Fig.-1.



Scheme-1: Three-Component Reaction for the Formation of the Target Molecule

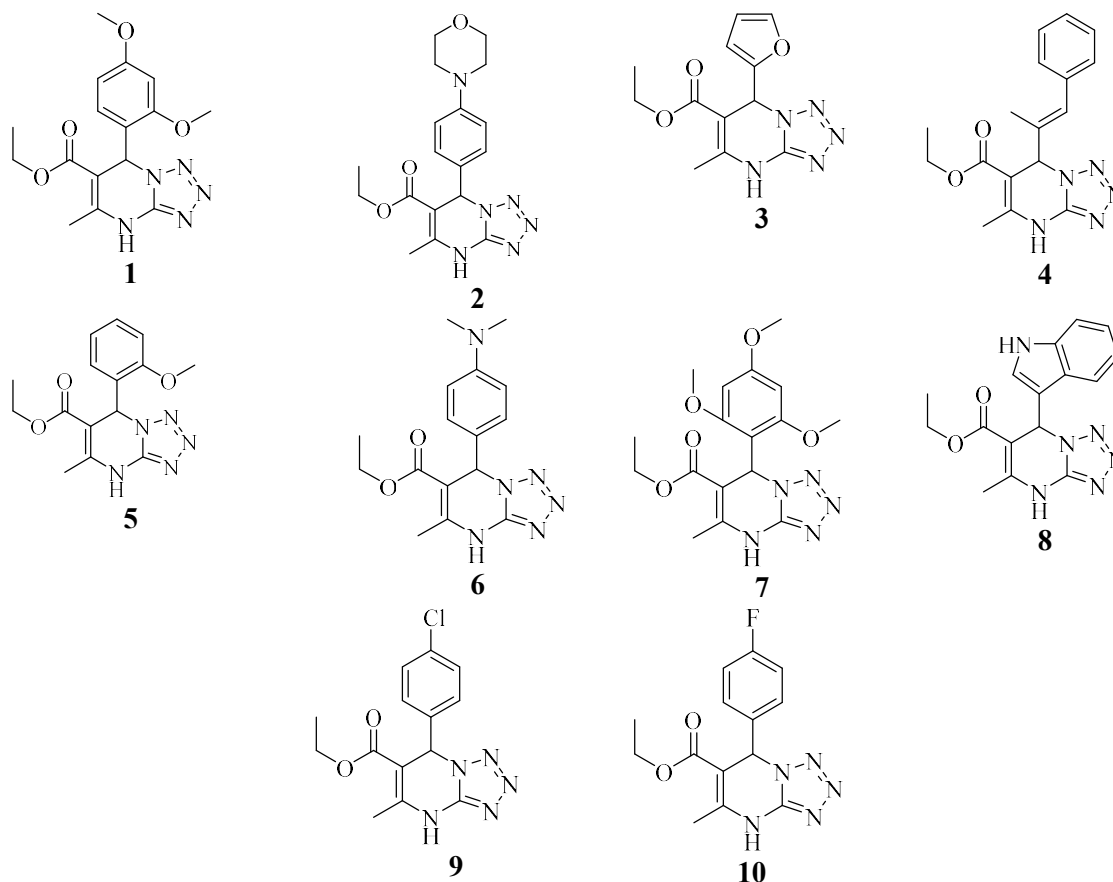


Fig.-1: Molecular Structure of the Synthesized Compounds

Three reaction mechanism pathways of the Biginelli reaction were already reported. Those were through Knoevenagel, enamine, and iminium routes.³⁹ However, reinvestigating the reaction mechanism conducted by Kappe³⁹ using NMR spectroscopy revealed that the reaction proceeded through the iminium route. Briefly, the reaction process proceeds as follows. The reaction starts with protonating aromatic aldehyde, followed by a nucleophilic attack of 5-amino tetrazole to form an iminium ion. The next step is a condensation of iminium ion with an enolate ion of ethyl-acetoacetate to form an intermediate as Knoevenagel product. Protonation of this intermediate leads to an intermediate, followed by intramolecular cyclization. Then dehydration and deprotonation steps lead to the target molecule.³⁹ The yield and reaction time of the target compounds are presented in Table-1. It is observed that the reaction proceeded between 3-11 hours and yielded 3.22-74.28%. Further observation showed that electron-donating substituents attached in phenyl ring at C-7 (compound 1-8) accelerated the reaction time (3-9 h), while electron-withdrawing one (compound 9,10) slowed down the reaction time (11 h). However, on the contrary, electron-donating substituents lowered the yield (3.22 - 58.19%), while electron-withdrawing one increased the yield (58.58 - 74.28%). This finding follows the theoretical concept of the reaction mechanism of the Biginelli reaction through the iminium route, which is formed through the reaction between benzaldehyde derivatives and urea. The electron-withdrawing substituents of benzaldehyde increase carbonyl benzaldehyde's electrophilicity, which accelerates the reaction.³⁶

Table-1: Yield and Reaction Time of the Synthesis of Target Molecules

No	Compound	Yield (%)	Time (h)
1	1	45.91	7
2	2	58.19	7
3	3	47.87	9
4	4	11.89	7

5	5	47.59	5
6	6	42.40	7
7	7	29.45	3
8	8	2.59	5
9	9	74.28	11
10	10	58.58	11

Compounds 2-7 and 9-10 were purified by recrystallization from a mixed solvent of ethanol-water, and compound 7 was recrystallized from ethanol. Compounds 1 and 8 were purified chromatographically using a silica column as stationary phase and a combination of ethyl acetate: dichloromethane (1:2) as mobile phase for compound 1 and chloroform: ethyl acetate (3:1) for compound 8. Based on SciFinder research, compounds 1 and 8 are commercially available, while compounds 4 and 7 are new. The synthesis and structure characterization of compound 2 has been reported previously in detail²⁸, while compounds 3, 5, 6, 9, and 10 are already reported previously. We determined the molecular structure of all prepared compounds based on HR-MS, FTIR, and NMR spectroscopic data. The HR-MS spectrum of the obtained exhibited conformity between the observed and calculated molecular mass. According to FTIR spectra, the vibration bands $\tilde{\nu}$ consecutively at range 3232-3335, 3161-3180, 2912-2956, 1676-1712, 1556-1577, 1095-1128, and 1217-1230 cm^{-1} are evidence for the existence of secondary N-H bond, C-H sp^2 , C-H sp^3 , C=O ester, C=C aromatic, and C-O ester respectively. A consistent pattern of the ^1H -NMR spectrum of all the prepared compounds was observed, which were singlet signals at δH 2.36-2.69 ppm represented methyl protons attached at C-5. The others singlet signals at δH 6.23-7.06 ppm are suitable for the chiral proton signal at C-7 of the purine ring of prepared compounds. The N-H appeared as singlet signals at δH 10.97-11.33 ppm. Moreover, these data were also supported by ^{13}C -NMR (APT) data, which exhibited the existence of C-5, C-5a, C-6, and C-7 signals that appeared consecutively at a range of δC 145.4-147.3, 148.3-149.5, 95.2-99.58, and 49.2-62.9 ppm. These data showed the existence of a purine ring of all target molecules.⁴¹

Bioactivities Evaluation

Cytotoxicity Activity in Vitro

A 3-(4,5-dimethylthiazol-2-yl)-2,5-diphenyltetrazolium bromide (MTT) colorimetric assay was applied to evaluate the antiproliferative activity of the prepared compounds toward human breast cancer cell line 4T1 and cervical cancer cell line HeLa, with doxorubicin as a positive control. The results were presented as growth inhibitory concentration (IC_{50}) values in Table-2.

The tested samples showed cytotoxic activity toward the two cancer cell lines used in this experiment. Although none of the tested compounds exhibited anti-proliferative activities on the order of the positive control doxorubicin, their activities ranged from strong (compounds 4 and 8) to moderate (compounds 1-3, 5-7, and 9-10). Compounds exhibiting $\text{IC}_{50} > 50 \mu\text{M}$ were not considered to have activity.³²

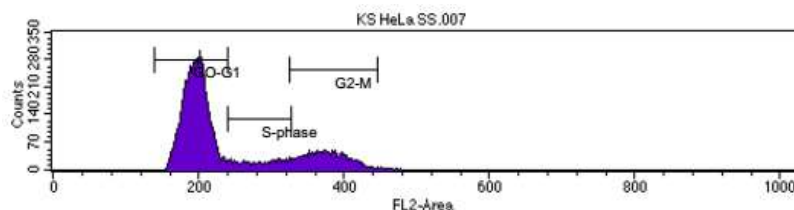
Table-2: *In vitro* Cytotoxicity of the Prepared Compounds

Sample	IC_{50} (μM)	
	4T1	HeLa
1	0.272	0.603
2	0.824	0.085
3	0.664	0.619
4	0.040	0.023
5	0.548	0.319
6	0.897	0.299
7	0.664	0.643
8	0.045	0.041
9	3.737	0.458
10	0.470	0.305
Doxorubicin	0.006	0.002

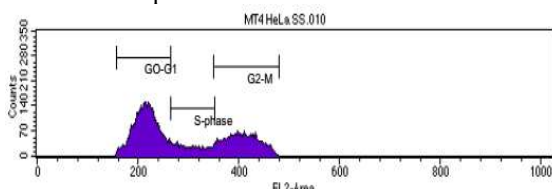
Cell Cycle Analysis

Considering their strong anti-proliferative activities, compounds 4 and 8 were tested for further biological activities. To obtain a deeper understanding of the cytotoxic activities of these compounds, their effects on the phases of the cell cycle and induction of apoptosis were appraised using 4T1 and HeLa cells according to a method outlined in the previous studies.¹⁷ Generally, anticancer agents inhibit the growth and multiplication of cancer cells by restraining cell division at certain checkpoints. Furthermore, cells that resist apoptosis are traditionally averse to cancer therapy.²⁰ Herein, HeLa cancer cell lines were treated with compounds 4 and 8 at concentrations equal to their IC₅₀ value from the above anti-proliferation assays (0.023 μ M for compound 4 and 0.041 μ M for compound 8) for 24 h.

a. Control



b. Compound 4



c. Compound 8

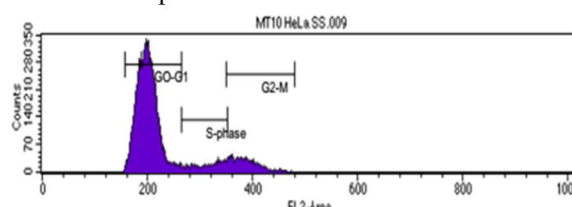


Fig.-2: HeLa Cancer Cell Line Distribution Upon Treatment with (a) Doxorubicin, (b) Compound 4, and (c) Compound 8

As shown in Fig.-2 and Table 2, the percentage of HeLa cells at the G0–G1 phase decreased from 70.61% to 53.69%, while that in the S phase increased from 9.40% to 13.52%, and that in G2–M, phase was enhanced from 20.26% to 33.50% after treatment with compound 4, indicating that compound 4 led to cell cycle arrest at G0–G1 phase. Furthermore, the percentage of HeLa cells in the G0–G1 phase increased from 70.61% to 81.00%, in the S phase decreased from 9.40% to 8.61%, and in the G2–M phase decreased from 20.26% to 10.97% after treatment with compound 8. This demonstrated that compound 8 led to cell cycle arrest at the G2–M phase.

Table-2: Effect of Compounds 4 and 8 on Cell Cycle Progression in HeLa Cancer Cells

Sample	Cell cycle distribution (%)		
	G0–G1	S	G2–M
Control	70.61	9.40	20.26
Compound 4	53.69	13.52	33.50
Compound 8	81.00	8.61	10.97

Annexin V-PI Apoptosis Assay

Determination of apoptosis induction effects of compounds 4 and 8 was made in cell lines HeLa via PI and Annexin V double staining assay after incubating cells for 24 h with compound 4 or 8 at concentrations equal to their previously determined IC₅₀ values, shown in Table-3 and Fig.-3.

Table-3: Percent of Apoptotic and Necrotic HeLa Cells Induced by Compound 4 or 8

Sample	Apoptosis (%)			
	Total	Early	Late	Necrosis
Control	93.56	0.85	2.75	2.92
Compound 4	68.51	3.50	18.46	9.98
Compound 8	1.97	0.03	6.09	91.97

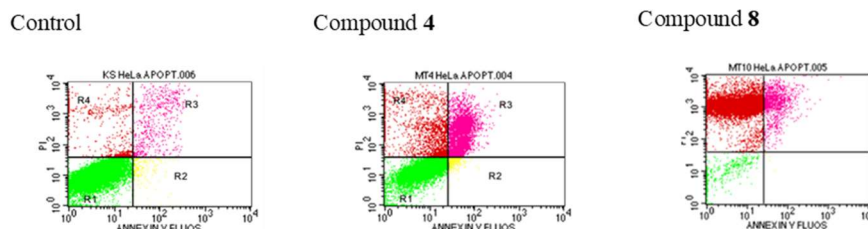


Fig.-3: Apoptosis of HeLa Cancer Cells Induced by Compounds 4 and 8

These results revealed that compound 4 induced early apoptosis in 3.50% of cells and increased late apoptosis by 18.46%, whereas compound 8 caused early apoptosis in 0.03% of cells and increased late apoptosis by 6.09%. On the other hand, 0.85% of untreated HeLa cells exhibited early apoptosis, and 2.75% exhibited late apoptosis. Unfortunately, compound 8 appeared to cause necrosis in 91.97% of cells.

Antidiabetic Activity

Diabetes mellitus (DM) is a complex chronic illness associated with hyperglycemia or a high blood glucose level, which occurs from a lack of insulin secretion action, or both.⁴² Therefore, all available anti-diabetic drugs considered the most effectively used in managing type-2 DM are designed as α -Glucosidase inhibitors. In this present study, the prepared compounds are designed as α -Glucosidase inhibitors. The results of antidiabetic activity assays of the prepared compounds are displayed in Table 4. The antidiabetic activities of the tested samples were calculated as percent inhibition (%) at 10 mg/ml and IC_{50} (mM). Quercetin, known to exhibit antidiabetic activity, was used as a control. Briefly, the tested compounds exhibited better inhibitory activity against maltase than sucrose at 10 mg/ml concentrations and their respective IC_{50} concentrations. In addition, compounds 4, 6, 7, and 9 exhibited better inhibitory activity even than quercetin against maltase, while compounds 7 and 8 showed better inhibitory activity than quercetin against sucrase.

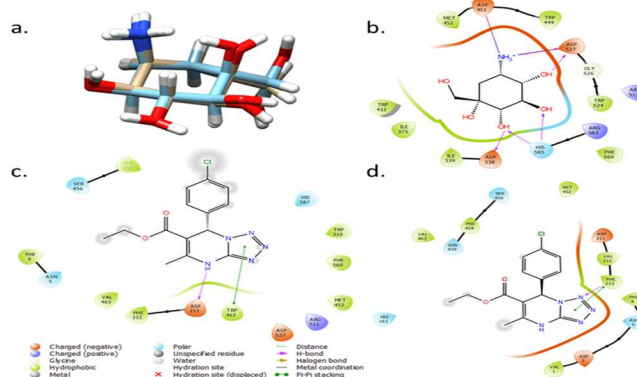
Table-4: Inhibition Activity of the Prepared Compounds Against α -glucosidase

No	Compounds	Molecular weight	Percentage inhibition (%) at 10 mg/mL		IC_{50} (mM)*	
			Maltase	Sucrase	Maltase	Sucrase
1	1	345.13	37.17	13.59	NI**	NI
2	2	371.18	22.77	26.64	NI	NI
3	3	275.10	32.90	17.82	NI	NI
4	4	325.15	61.17	19.35	1.67	NI
5	5	315.13	17.12	32.92	NI	NI
6	6	328.16	53.60	15.26	1.83	NI
7	7	375.15	46.77	42.83	1.67	1.67
8	8	324.13	19.60	55.24	NI	1.51
9	9	319.08	75.26	14.83	0.85	NI
10	10	303.11	22.34	3.20	NI	NI
11	Quercetin		-	-	2.72	1.76

*Nonlinear regression analyses were conducted in SigmaPlot 12.5; ** NI, no inhibition, inhibitory effect less than 40% at 10 mg/ml

As presented in Table 4, compound 7 showed better inhibitory activity against maltase and sucrase, so that used to study the inhibitory mechanism of the tested compound by observing its intermolecular interaction in silico with α -glucosidase (PDB: 7K9Q) and compared with valioline as ligand. Based on the result of pose reproduction, the computed grid successfully predicted the crystallographic pose of valioline as cognate ligands (HA_RMSDh = 0.6613), as shown in Scheme-2. The calculated docking score of valioline, *R*- and *S*-DHPM-7 are -50.13; -32.23; and -30.83, respectively. Obtained all grid score of DHPM-7 is more positive than valioline, indicating this compound is predicted to have less affinity or inhibition. Valioline has six interactions; four are hydrogen bonds, and the others are electrostatic interactions (Scheme-2b). Since the catalytic residue is anionic, the amine group in valioline plays a

pivotal role in affinity by electrostatic interaction. Differing from valiolumine, DHPM-7 has only two interactions: hydrogen bond and van der Waals interaction (π -stacking).



Scheme-2: Superimpose of Crystallographic and Docking Pose of Valiolamine (a), Interaction Binding Site with Valiolamine (b), S-DHPM-7 (c) dan R-DHPM-7 (d)

CONCLUSION

In conclusion, we have successfully synthesized 10 dihydrotetrazolopyrimidine derivatives *via* the Biginelli reaction. The synthesized compounds exhibited strong and moderate anti-proliferative activities against 4T1 and HeLa cancer cell lines *via* induction of apoptosis. Some tested compounds showed inhibitory activities against rat intestinal α -glucosidase superior to the positive control quercetin.

ACKNOWLEDGMENTS

This research was funded by the Ministry of Research and Technology/ National Agency for Research and Innovation through the "Hibah Penelitian Dasar Unggulan Perguruan Tinggi" research grant 2019

CONFLICT OF INTERESTS

The authors declare that there is no conflict of interest.

AUTHOR CONTRIBUTIONS

All the authors contributed significantly to this manuscript, participated in reviewing/editing, and approved the final draft for publication. The research profile of the authors can be verified from their ORCID ids, given below:

Hery Suwito <http://orcid.org/0000-0002-5844-067x>

N. Kurnyawati <http://orcid.org/0000-0002-4022-6886>

K. Ul Haq <http://orcid.org/0000-0002-0584-5040>

R.Ramadhan <http://orcid.org/0000-0002-2565-7944>

A. Abdulloh <http://orcid.org/0000-0001-9149-2028>

P. Phuwapraisirisan <http://orcid.org/0000-0001-6481-7712>

H.D. Hardiyanti <https://orcid.org/0000-0003-3196-6310>

Open Access: This article is distributed under the terms of the Creative Commons Attribution 4.0 International License (<http://creativecommons.org/licenses/by/4.0/>), which permits unrestricted use, distribution, and reproduction in any medium, provided you give appropriate credit to the original author(s) and the source, provide a link to the Creative Commons license, and indicate if changes were made.

REFERENCES

1. M.C. Harding, C.D. Sloan, R.M. Merrill, T.M. Harding, B.J. Thacker, E.I. Thacker, *Preventing Chronic Disease*, **15**, E158(2018), <https://doi.org/10.5888/pcd15.180151>
2. American Cancer Society, Cancer Facts and Figures 2022.

3. I. Miladiyah, E. Yuanita, S. Nuryadi, J. Jumina, S.M. Haryana, M. Mustofa, *Current Therapeutic Research*, **92**, 10057 (2020), <https://doi.org/10.1016/j.curtheres.2020.100576>
4. R. Nishimura, R. K. Tabata, M. Arakawa, Y. Ito, Y. Kimura, T. Akihasa, H. Nagai, A. Sakuma, H. Kohno, T. Suzuki, *Biological Pharmaceutical Bulletin*, **30**, 10(2007), <https://doi.org/10.1248/bpb.30.1878>
5. S.T. Diepstraten, M.A. Anderson, P.E. Czabotar, G. Lessene, A. Strasser, G.L. Kelly, *Nature Reviews Cancer*, **22**, 45(2022), <https://doi.org/10.1038/s41568-021-00407-4>
6. H. Sun, P. Saeed, S. Karuuanga, M. Pinkepank, K. Ogurtsova, B.B. Duncan, C. Stein, A. Basit, J.C.N. Chan, J.C. Mbanya, M.E. Packov, A. Ramachandaran, S.H. Wild, S. James, W.H. Herman, P. Zhang, C. Bommer, S. Kuo, E.J. Boyko, D.J. Magliano, *Diabetes Research and Clinical Practice*, **183**, 109119(2022), <https://doi.org/10.1016/j.diabres.2021.109119>
7. M. Fan, Q. Feng, M. He, W. Yang, Z. Peng, Y. Huang, G. Wang, *Arabian Journal of Chemistry*, **15**, 104301(2022), <https://doi.org/10.1016/j.arabjc.2022.104301>
8. N.M. Saleh, M.G. El-Gazar, H.M. Aly, R.A. Othman, R.A. *Frontiers in Chemistry*, **7**, 917(2020), <https://doi.org/10.3389/fchem.2019.00917>
9. R. Yousefi, M. Alavian-Mehr, F. Mokhtari, F. Panahi, M.H. Mehraba, A. Khalafi-Nezhad, *Enzyme Inhibition and Medicinal Chemistry*, **28**, 6(2013), <https://doi.org/10.3109/14756366.2012.727812>
10. B.K. Tripathi, A.K. Srivasta, *Medical Science Monitor*, **12**, 7(2006), <https://doi.org/10.12659/MSM.939088>
11. World Health Organization (WHO): Diabetes Mellitus, (1999).
12. M.A. Grillo, S. Colombatto, *Amino Acids*, **35**, 1(2008), <https://doi.org/10.1007/s00726-007-0606-0>
13. C. Carina Proenc, M. Freitas, D. Ribeiro, E.F.T. Oliveira, J.L.C. Sousac, S.M., Tome, M.J., Ramosb, A.M.A. Silvac, P.A. Fernandes, E. Fernandes, *Journal of Enzyme Inhibition and Medicinal Chemistry*, **32**, 1(2017), <https://doi.org/10.1080/14756366.2017.1368503>
14. S. Bajaj, A. Khan, *Indian Journal of Endocrinology and Metabolism*, **16**, 2(2012), <https://doi.org/10.4103/2230-8210.104057>
15. S. Shiyani, F. Arimia, G. Pratiwi, *Rasayan Journal of Chemistry*, **13(3)**, 1472(2020), <https://doi.org/10.31788/RJC.2020.1335755>
16. K.B. Pandeya, *International Journal of Organic Chemistry*, **3**, 1(2013), <https://doi.org/10.4236/ijoc.2013.31001>
17. X. Liu, L. Zhu, J. Tan, X. Zhou, L. Xiao, X. Yang, B. Wang, *BMC Complementary Medicine and Therapies*, **14**, 1(2014), <https://doi.org/10.1186/1472-6882-14-12>
18. W. Hakamata, M. Muroi, T. Nishio, T. Oku, A. Takatsuki, H. Osada, K. Fukuhara, H. Okuda, M. Kurihara, *Journal of Applied Glycoscience*, **53**, 149(2006), <https://doi.org/10.5458/jag.53.149>
19. K. Okada, T. Yanagawa, E. Warabi, K. Yamatsu, J. Uwayama, K. Takeda, H. Utsunomiya, H. Yoshida, J. Shoda, T. Ishii, *Hepatol Res.*, **39**, 490(2009), <https://doi.org/10.1111/j.1872-034X.2008.00478.x>
20. L. Zeng, G. Zhang, S. Lin, D. Gong, *Journal of Agricultural and Food Chemistry*, **64**, 6939(2016), <https://doi.org/10.1021/acs.jafc.6b02314>
21. L. Zhang, Q. Chen, L. Li, *Scientific Reports*, **6**, 32649(2016), <https://doi.org/10.1038/srep32649>
22. J.H. Clark, D.J. Macquarrie, J. Sherwood, *Chemistry A European Journal*, **19**, 16(2013), <https://doi.org/10.1002/chem.201204396>
23. J.J. Li, *Name Reactions: A Collection of Detailed Mechanisms and Synthetic Applications*, Springer International Publishing, New York, p. 42-43 (2014)
24. V.L. Gein, T.M. Zamaraeva, N.V. Nosova, M.I. Vakhrin, P.A. Slepukhin, *Russian Journal of Organic Chemistry*, **48**, 5(2012), <https://doi.org/10.1134/S107042801203013X>
25. V.L. Gein, T.M. Zamaraeva, M.I. Vakhrin, *Pharmaceutical Chemistry Journal*, **44**, 7(2010), <https://doi.org/10.1007/s11094-010-0469-7>
26. V.P. Gilava, P.K. Patel, H.K. Ram, J.H. Chauhan, *Rasayan Journal of Chemistry*, **13(4)**, 2249(2020), <https://doi.org/10.31788/RJC.2020.1346072>
27. V.L. Gein, T.M. Zamareva, V.V. Mishunin, V.P. Kotegov, V.P. *Russian Journal of General Chemistry*, **86**, 286(2016), <https://doi.org/10.1134/S1070363216020134>

28. A. Haleel, D. Mahendiran, V. Veena, N. Sakthiel, A.K. Rahiman, *Materials Science and Engineering: C*, **68**, 366(2016), <https://doi.org/10.1016/j.msec.2016.05.120>
29. S.B. Rathod., M.K. Lande, *Rasayan Journal of Chemistry*, **14(1)**, 368(2021), <https://doi.org/10.31788/RJC.2021.1416121>
30. J. Gao, X. Liu, B. Zhang, Q. Mao, Z. Zhang, Q. Zou, X. Dai, S. Wang, *European Journal of Medicinal Chemistry*, **190**, 112077(2020), <https://doi.org/10.1016/j.ejmech.2020.112077>
31. H. Suwito, N. Kurnyawaty, K. Ul Haq, A. Abdulloh, I. Indriani, *Molbank*, **M998**, (2018), <https://doi.org/10.3390/M998>
32. A.M. El-Naggar, M.M. Hemden, S.R. Atta-Allah, *Journal of Heterocyclic Chemistry*, **54**, 3519(2017), <https://doi.org/10.1002/jhet.2975>
33. F. Denizot, R. Lang, *Journal of Immunological Methods*, **89**, 271(1986), [https://doi.org/10.1016/0022-1759\(86\)90368-6](https://doi.org/10.1016/0022-1759(86)90368-6)
34. S. Zhang, T. Li, L. Zhang, X. Wang, H. Dong, L. Li, D. Fu, Y. Li, X. Zi, H. Liu, Y. Zhang, H. Xu, C-Y. Jin, C-Y, *Scientific Reports*, **7**, 9873(2017), <https://doi.org/10.1038/s41598-017-10400-3>
35. T. Mosmann, *Journal of Immunological Methods*, **65**, 55(1983), [https://doi.org/10.1016/0022-1759\(83\)90303-4](https://doi.org/10.1016/0022-1759(83)90303-4)
36. R. Ramadhan, P. Phuwapraisirisan, P, *Natural Product Communication*, **10(2)**, 325(2015)
37. S.S. Karade, M.L. Hill, J.L. Kiappes, R. Manne, B. Aakula, N. Zitzmann, K.L. Warfield, A.M. Treston, and R.A. Mariuzza, *Journal of Medicinal Chemistry*, **64**, 18010(2021), <https://doi.org/10.1021/acs.jmedchem.1c01377>
38. E.F. Pettersen, T.D. Goddard, C.C. Huang, G.A. Couch, D.M. Greenblatt, E.C. Meng, and T.E. Ferrin, *Journal of Computational Chemistry*, **25**, 1605(2004), <https://doi.org/10.1002/jcc.20084>
39. W.J. Allen, T.E. Balius, S. Mukherjee, S.R. Brozell, D.T. Moustakas, P.T. Lang, D.A. Case, I.D. Kuntz, and R.C. Rizzo, *Journal of Computational Chemistry*, **36**, 1132(2015), <https://doi.org/10.1002/jcc.23905>
40. M.D. Hanwell, D.E. Curtis, D.C. Lonie, T. Vandermeersch, E. Zurek, and G.R. Hutchison, *Journal of Cheminformatics*, **4**, 17(2012), <https://doi.org/10.1186/1758-2946-4-17>
41. A. Jakalian, D.B. Jack, C.I. Bayly, *Journal of Computational Chemistry*, **23**, 1623(2002), <https://doi.org/10.1002/jcc.10128>
42. C.O. Kappe, *The Journal of Organic Chemistry*, **62**, 7201(1997), <https://doi.org/10.1021/jo971010u>
43. H. Nagarajaiah, A. Mukhopadhyay, J.N. Moorthy, *Tetrahedron Letters*, **57**, 47(2016), <https://doi.org/10.1016/j.tetlet.2016.09.047>
44. D.L. Pavia, G.M. Lampman, G.S. Kriz, J.R. Vyvyan, J.R, 2014, *Introduction to Spectroscopy*, Brooks/Cole, Belmont –USA, p.233-293 (2014)
45. A. Chaudhury, C. Duvoor, V.S.R. Dendi, S. Kraleti, A. Chada, R. Ravilla, A. Marco, N.S. Shekhawat, M.T. Montales, K. Kuriakose, A. Sasapu, A. Beebe, N. Patil, C.K. Musham, G.P.Lohani, W. Mirza, *Frontiers in Endocrinology*, **8**, 6 (2017), <https://doi.org/10.3389/fendo.2017.00006>

[RJC-8025/2022]